

## A simple vibrating sample magnetometer for macroscopic samples

V. Lopez-Dominguez, A. Quesada, J. C. Guzmán-Mínguez, L. Moreno, M. Lere, J. Spottorno, F. Giacomone, J. F. Fernández, A. Hernando, and M. A. García

Citation: [Review of Scientific Instruments](#) **89**, 034707 (2018); doi: 10.1063/1.5017708

View online: <https://doi.org/10.1063/1.5017708>

View Table of Contents: <http://aip.scitation.org/toc/rsi/89/3>

Published by the [American Institute of Physics](#)

---

### Articles you may be interested in

[Contributed Review: Camera-limits for wide-field magnetic resonance imaging with a nitrogen-vacancy spin sensor](#)

[Review of Scientific Instruments](#) **89**, 031501 (2018); 10.1063/1.5010282

[Simple and portable low frequency lock-in amplifier designed for photoacoustic measurements and its application to thermal effusivity determination in liquids](#)

[Review of Scientific Instruments](#) **89**, 034904 (2018); 10.1063/1.4997455

[Quasi-adiabatic calorimeter for direct electrocaloric measurements](#)

[Review of Scientific Instruments](#) **89**, 034903 (2018); 10.1063/1.4997155

[Relaxation calorimetry at very low temperatures for systems with internal relaxation](#)

[Review of Scientific Instruments](#) **89**, 033908 (2018); 10.1063/1.5018739

[Error analysis and new dual-cosine window for estimating the sensor frequency response function from the step response data](#)

[Review of Scientific Instruments](#) **89**, 035002 (2018); 10.1063/1.5001689

[New design for inertial piezoelectric motors](#)

[Review of Scientific Instruments](#) **89**, 033704 (2018); 10.1063/1.5008471

---

**Scilight**

Sharp, quick summaries **illuminating**  
the latest physics research

Sign up for **FREE!**

**AIP**  
Publishing

## A simple vibrating sample magnetometer for macroscopic samples

V. Lopez-Dominguez,<sup>1,2,3</sup> A. Quesada,<sup>1</sup> J. C. Guzmán-Mínguez,<sup>1</sup> L. Moreno,<sup>1</sup> M. Lere,<sup>4</sup> J. Spottorno,<sup>2</sup> F. Giacomone,<sup>2</sup> J. F. Fernández,<sup>1</sup> A. Hernando,<sup>2</sup> and M. A. García<sup>1,2,a)</sup>

<sup>1</sup>Instituto de Cerámica y Vidrio–Consejo Superior de Investigaciones Científicas, Madrid, Spain

<sup>2</sup>Instituto de Magnetismo Aplicado–UCM-ADIF, Unidad Asociada CSIC, Madrid, Spain

<sup>3</sup>Department of Electrical Engineering and Computer Science, Northwestern University, 2145 Sheridan Rd., Evanston, Illinois 60208, USA

<sup>4</sup>Instituto de Investigación en Ciencia y Tecnología de Materiales, CONICET, Mar del Plata, Buenos Aires, Argentina

(Received 29 November 2017; accepted 10 March 2018; published online 28 March 2018)

We here present a simple model of a vibrating sample magnetometer (VSM). The system allows recording magnetization curves at room temperature with a resolution of the order of 0.01 emu and is appropriated for macroscopic samples. The setup can be mounted with different configurations depending on the requirements of the sample to be measured (mass, saturation magnetization, saturation field, etc.). We also include here examples of curves obtained with our setup and comparison curves measured with a standard commercial VSM that confirms the reliability of our device. *Published by AIP Publishing.* <https://doi.org/10.1063/1.5017708>

### INTRODUCTION

Magnetic materials are ubiquitous nowadays due to their massive use in energy management, data storage, technological devices, transportation, biomedicine, or environmental protection.<sup>1–3</sup> Therefore, the measurement of magnetic properties, and in particular magnetization curves, is essential for both fundamental and applied research. Among the different types of magnetometers, the Vibrating Sample Magnetometer (VSM) developed by Simon Foner<sup>4–7</sup> is particularly appealing due to its simplicity and versatility, and, consequently, it is one of the most common systems for the characterization of magnetic materials. The VSM does not require superconductors, cryogenic elements such as superconducting quantum interference devices (SQUIDS), nor the application of AC magnetic fields (as it is the case of standard induction systems) that limits the maximum achievable field. Following pioneering Foner's work, a large number of configuration and improvements for the VSM have been proposed.<sup>8–14</sup>

Nowadays there are a large number of commercial VSMs that allow both reaching sensitivity of  $10^{-6}$  emu and variable temperature. This resolution is certainly required for the study of nanometric systems as thin films. However, such resolution may not be required for the study of a large number of materials. For instance, a steel sample with  $1 \text{ mm}^3$  volume exhibits a magnetic moment of the order of 1 emu. Similarly, ferrites exhibit saturation magnetization of the order of 10–80 emu/g, so a sample with 50 mg presents a saturation magnetization of  $\sim 1$  emu.

We present here a particular model of VSM which is easy to fabricate and versatile. Our setup is simple, providing a full automatic control of the measurement process and data acquisition with a single computer connection.

The pick-up coils are designed to enhance sensitivity irrespective of the sample geometry and they are planar, thus allowing us to reduce the gap between the electromagnet poles and consequently, achieving larger magnetic fields at the sample space.

The scheme of the system is depicted in Fig. 1 and follows the configuration of the classical VSM. A vertical vibration head is placed on top of the system and connected to a rod that holds the sample at its bottom end. An electromagnet is placed to create a horizontal magnetic field at the sample space. Pick-up coils are placed between the electromagnet poles and the sample. The signal detected at the coils is transmitted through a coaxial cable to a lock-in amplifier tuned at the frequency of the sample vibration. The system is controlled by a computer that allows varying the magnetic field created by the electromagnet and measuring the signal induced at the pick-up coils. In this way, magnetization curves can be recorded at room temperature. We describe here each of these elements.

### LOCK-IN AMPLIFIER

The core of the system is a dual phase lock-in amplifier SRS830 from *Stanford Research System*. Besides allowing to measure AC signals of the order of 10 nV, it has additional useful advantages for the control of the auxiliary systems. AC reference signals (from 0.1 Hz to 100 KHz) can be internally generated and provided an output with variable amplitude between 0 and 5 V to feed the vibrating head. Auxiliary input and output ports are used for generating and measuring DC signals in the range  $-10$  to 10 V for the control and measurement of the applied magnetic field. Dual lock-in amplifiers can measure the module of the induced signal (i.e., the R value), thus cancelling the effect of dephasing between the reference signal provided by the lock-in amplifier for the vibration and the induced signal.

<sup>a)</sup> Author to whom correspondence should be addressed: [magarcia@icv.csic.es](mailto:magarcia@icv.csic.es)

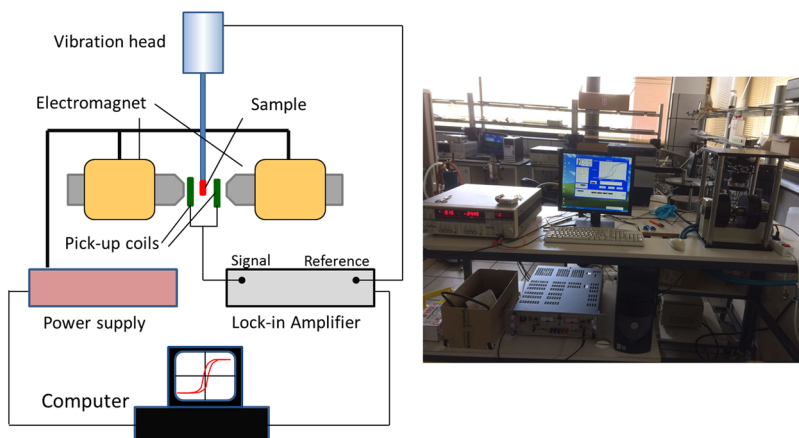


FIG. 1. Scheme and photo of the designed VSM.

### VIBRATING HEAD AND MECHANICAL STRUCTURE

The vibrating head is a vibrating Generator 2185.00 from *Frederiksen Ltd.* This head is basically a loudspeaker that can generate a mechanical vibration with frequencies in the range 0.1 Hz–5 kHz. The maximum amplitude vibration is 7 mm at 1 Hz, decreasing with increasing frequency. The input impedance of the head is  $8\ \Omega$  and the input signal is limited to 6 V/1 A. As the internal frequency generator of the SRS830 lock-in amplifier provides an output signal up to 5 V in the range 0.1 Hz–100 KHz, it can be used to directly feed the vibrating head. A rod is fixed to the vibrating element and the sample is placed at the end of the rod. The rod must be fabricated on a rigid, diamagnetic and insulating material. Glass fiber is a good choice. We also tested Polyvinyl Chloride (PVC) and other plastics which were easier to mechanize and the results were satisfactory for vibration frequencies below 350 Hz.

The mechanical structure is that shown in Fig. 2. The vibrating head is fixed to a translation stage to allow displace-

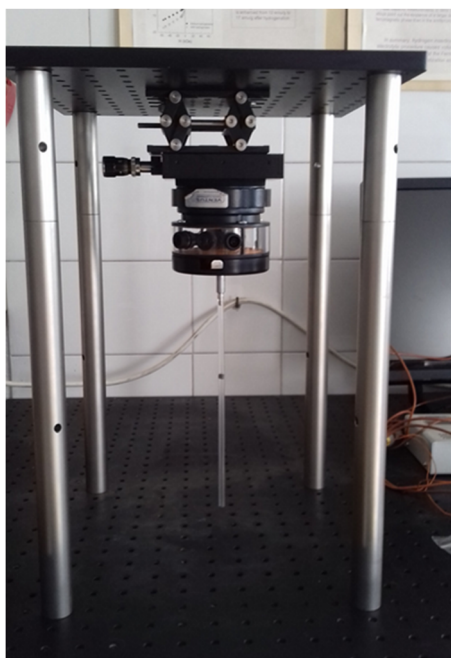


FIG. 2. Photo of the mechanical structure.

ments in the three spatial dimensions [formed by two PT1 for the X and Y directions (horizontal plane) and one L200 for the Z direction (vertical), all from *Thorlabs*]. The translation stage is fixed to a platform suspended on four pillars and attached to the base. All the elements are metallic and have a large weight and reduce the vibration of the structure, increasing the mechanical stability of the system. Note that the ratio of vibration amplitudes of the vibrating element of the head and the rest of the system will be inversely proportional to the ratio of its masses. In our case, the weight of the upper platform, translation stage, pillars, and base was 11.4 kg. As the weight of the vibrating element with the rod and the sample is of the order of  $\sim 10$  g, for a vibrating amplitude of the sample of 5 mm, the rest of the system vibrates with an amplitude of  $\sim 5\ \mu\text{m}$ . If possible, this structure must be mechanically isolated from the electromagnet and pick-up coils to further increase the mechanical stability.

### MAGNETIC FIELD SOURCE

The magnetic field source of the VSM must fulfill two requirements:

- The magnetic field must be enough to saturate the studied samples. Otherwise, we will obtain minor loops that are not representative of the material and can lead to erroneous results about the magnetic properties of the material.
- The magnetic field must be uniform at the sample space (including the vibration space). Otherwise, field gradients will induce forces that may alter the vibration leading to erroneous results. In addition, inhomogeneous fields may lead to false values of the applied field and consequently, distorted magnetization curves.

Two types of magnetic sources can be used to this purpose, electromagnets or coils, both connected to a current source. We will analyze both cases separately.

### ELECTROMAGNET

Electromagnets allow reaching larger magnetic fields than coils but the spatial uniformity is limited to a small region.

Actually, this region will not depend only on the electromagnet but also on the poles distance and faces.

Any standard electromagnet can be used to fabricate the VSM provided that it produces a uniform field in the sample space (including the vibration region). The power supply for the electromagnet must be bipolar to obtain magnetization curves in a fully automatized mode. It also must allow external control of the current with an input voltage (preferably in the range  $-10$  to  $10$  V).

In our systems, we use an electromagnet model 3470 from *GMW Associates* with cylindrical poles. It allows reaching 1 T field with 1 cm gap between poles (using 20 mm face poles) for a current of 5 A. The power supply was a BOP 50-8ML from *KEPCO* (50 V, 8 A, bipolar) that includes the above-mentioned external control. Hence, the control of the current is performed by using the auxiliary output ports of the lock-in amplifier to place a  $\pm 10$  V signal on the current control of the source.

The distance between poles and their face diameter must be chosen with a compromise between the field uniformity and intensity. For instance, with 20 mm diameter poles, the stability of the field in the horizontal direction is better than 0.5% in a 5 mm region, while using 40 mm poles, this stability reaches 15 mm. On the contrary, the maximum achievable field is about 20% larger with the 20 mm poles than with the 40 mm ones.<sup>15</sup>

## COILS

Coils produce smaller fields than electromagnets but, with an appropriated configuration, they provide better field uniformity than electromagnets. The best configuration corresponds to Helmholtz coils.<sup>16</sup> For this geometry, in which the distance between coils is equal to its radius, the first and second derivatives of the field with the displacement in the coils axis is zero at the sample position, leading to a better field uniformity.

Hence, for soft magnetic materials that require low magnetic field to saturate, the electromagnet can be replaced by Helmholtz coils to improve field uniformity.

## PICK-UP COILS

The design of the pick-up coils is the most critical step of the fabrication of VSMs. This design must combine several goals:

- Maximize the induced signal, in order, to improve the sensibility of the VSM.
- Reduce the noise, especially that associated with fluctuations of the applied magnetic field, to increase the signal-to-noise ratio.
- Provide a wide saddle point at the sample space to make the measurements weakly sensitive to sample positioning error.
- Minimize the volume, to allow closing the gap, when an electromagnet is used, to achieve larger and more uniform magnetic fields at sample space.

Consequently, a large number of studies have addressed the problem of pick-up coils' design<sup>5,17-20</sup> and several configurations of coils can be used depending on the type of materials to be studied.

In our case, we prioritize the reduction of the noise and to increase the magnetic field achievable at the sample space. To this purpose, we designed a set of four planar coils. Using just two coils in the XZ plane and aligned with the center of the electromagnet poles [Fig. 3(a)], the vibration of the sample in the Z-direction will produce the same variation of flux in both coils. Thus, the signals from both coils must be added. In this configuration, any fluctuation of the applied magnetic field in the Y-direction created by the electromagnet will also induce identical signals in both coils. Hence, the instabilities of the applied magnetic field will increase the noise in the measured signal. An alternative approach should be shifting vertically the coils to have a configuration as that shown in Fig. 3(b). In this case, if the sample vibration amplitude is smaller than the vertical shift of the coils, the induced signal upon sample displacement in the Z-direction will be opposite for both coils and the signals should be subtracted. On the contrary, the signals induced by the applied magnetic field instability in the Y-direction will be the same for both coils and when the signals from both coils are subtracted, it is cancelled. The main disadvantage of this system is that from a geometrical point of view, it is highly asymmetric, so any non-symmetric instability of the field or vertical vibrations transmitted from the vibration head to the rest of the system will generate additional noise. In addition, non-symmetric samples (or not properly aligned) will induce signals hard to calibrate. The problem can be solved using a four-coil system as that presented in Fig. 3(c). The signal of opposite coils is subtracted (A-B) and (D-C) and the result is added. In this way, we have a symmetric pick-up coil system, where the contribution of the magnetic field instabilities is cancelled.

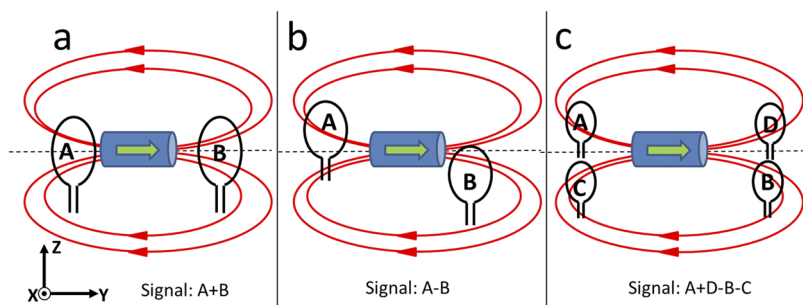


FIG. 3. Scheme of the different configurations of coils and the magnetic flux.

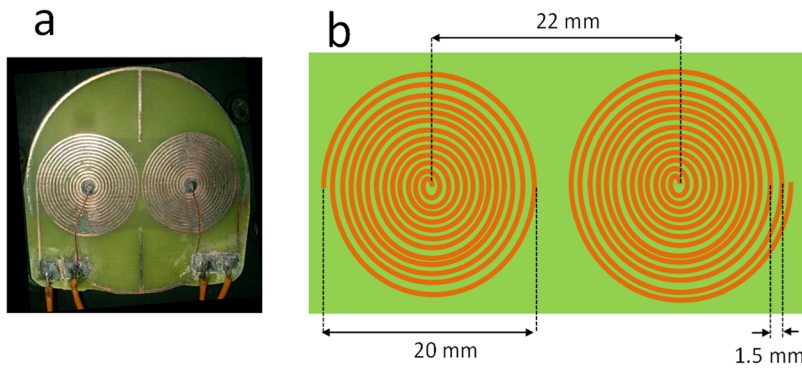


FIG. 4. (a) Photo and (b) scheme of the pick-up coils with dimensions.

In the VSM configuration shown in Fig. 1, the pick-up coils are placed between electromagnet poles and the sample. Therefore, using coils with a large number of turns requires a large space in the Y-direction, so the poles of the electromagnet must be separated, hence reducing the achieved magnetic field at the sample space. To minimize this space, we designed planar pick-up coils with spiral structure as shown in Fig. 4. The coils were printed by chemical etching on a single side prototyping board (AAC20 from C.I.F.) composed by the following stacks: a FR4 substrate, a thin copper film (33  $\mu\text{m}$  of thickness), and a photosensitive resin. The coil pattern was fabricated using a standard lithography process for electronics: first printed on a photographic slide and transferred to the board by illuminating with ultraviolet light (UV) during 2 min. After this process, the board is immersed in a solution of sodium metasilicate to remove the resin exposed to the UV light. Finally, the copper without the resin layer is attacked with a solution of chloride acid for 10 min. Once the coils are printed on the board, the excess of resin is cleaned from the board by acetone. The coils have a wire from the center to the edge of the board, to allow their connection. The signal from each coil is connected to wires that are braided until connected between them to produce the addition and subtraction of signals above described and then they are transmitted via a coaxial cable to the input of the lock-in amplifier. Coating the coils with kapton or any other transparent adhesive avoids oxidation and protects the coils from mechanical damage. Figure 4 shows a scheme and a photograph of the coils.

This planar structure limits the number of coil turns to a maximum of  $\sim 10\text{--}30$  depending on the patterning process,

a number is significantly smaller than those typically in non-planar coils (100–1000). However, the optimum diameter of the turns to maximize the induction upon sample vibration depends on the sample geometry and distance to the coil, which is an advantage for spiral structures.

To analyze this point, we calculated the induced voltage upon 1 mm amplitude vibration of the sample depending on the sample size, turns, radius, and sample-coil distance. Figure 5 illustrates the results.

The calculations show that depending on the coils-sample distance, the maximum sensitivity corresponds to a turn with different radius. At short distance (5 mm), the smaller turns provide the maximum induced signals, while for distances above 10 mm, larger coils register the maximum induction. Hence, the spiral coils will always have some turns which register a measurable signal irrespective of the sample-coil distances. The total induced signal will be larger for small distances ( $\sim 5$  mm) although in this case, the system must be calibrated with the same exact distance to avoid errors. On the contrary, for larger distances, the induced signal is reduced but it does not depend so strongly on the distance and calibration is not so critical. Hence, the optimum measurement conditions should be to measure with sample-coil distances of the order of 10–15 mm and, if the signal is too weak, to reduce this distance.

### CALIBRATION

The calibration of the magnetic moment is performed by using a sample with known saturation magnetization. The sample is placed in the VSM and a magnetic field strong enough

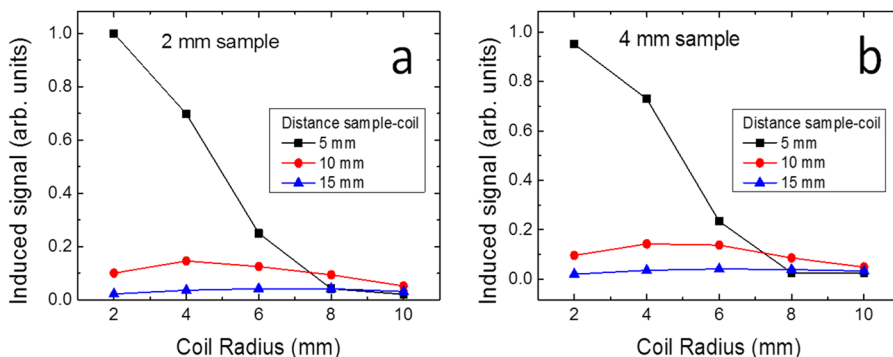


FIG. 5. Induced signal for individual turns in the pick-up coils upon 1 mm amplitude vibration depending on the turn radius and sample to coil distance.

to saturate the sample is applied. Then, the signal induced in the lock-in amplifier is measured and the calibration factor obtained. It is appropriated to saturate the samples with magnetic fields in both directions and obtain the average value of the induced signal to avoid errors due to any offset signal. It is also essential to check the dependence of the calibration factor with the sample geometry. Note that, as above indicated, when reducing the gap between the poles of the electromagnet, the proximity between the sample and the pick-up coils will make the calibration factor very sensitive to sample geometry.

As concerns calibration of the magnetic field, it is performed by applying a certain current and measuring the magnetic field at the sample space with a Hall probe. If possible, it is recommended to measure the magnetic field for different currents (in both directions) and check there is a linear relationship, obtaining the calibration factor from the slope of the curve.

## SOFTWARE

The software for the control of the system was developed in VISUAL BASIC. It uses a single connection via RS232 to the SRS830 lock-in amplifier. This connection allows measuring the signal, controlling the current of the power supply via auxiliary output ports, and modifying the vibration frequency or amplitude. The system allows selecting the parameters of the magnetization curves as maximum current and step of the measurements. The delay before measuring when the magnetic field is modified can be also set (note that this value must be at least five times the time constant of the lock-in amplifier). The interface also has a control panel of the lock-in amplifier to modify remotely the measurement conditions as shown in Fig. 6. It also allows generating a magnetic field and measuring the signal at the lock-in amplifier which results useful for tests and selecting measurement conditions.

The raw data obtained when measuring magnetization curves correspond to values of induced voltages at the pick-up coils as a function of the current through the electromagnet. To translate those values into magnetic moment vs applied magnetic field values, calibration factors must be applied as above described. The software includes two calibration windows to state these values. Then, the saved data contain the measured raw values (current, voltage) and the magnetic parameters (applied magnetic field, magnetic moment).

In our system, the applied magnetic field is nominal, i.e., it is calculated from the applied current. Alternatively, the magnetic field can be monitored *in situ* during measurements. To this purpose, a Hall probe must be placed permanently close to the sample position. When recording the magnetization curve, for each point, the magnetic field is measured. If the Hall system provides an analog output proportional to the magnetic field within the range 10 to  $-10$  V, it can be connected to the auxiliary input ports of the lock-in amplifier, so no additional connection to the computer is needed to record it. In our case, we developed a system with this option using a Hall probe, model FH 55 from *Magnet Physik*. This system provides an output analog signal of 3 V for full scale that can be read through the auxiliary ports of the lock-in amplifier. A window at the software interface is added to indicate the scale of the Hall probe, thus providing the calibration factor for the real applied magnetic field.

Three VSMS following this configuration have been fabricated and they are working nowadays at the filiations of the authors of this paper. We present here a magnetization curve measured at room temperature with the magnetometer installed in filiation 1 of this paper (Instituto de Cerámica y Vidrio-CSIC) and with a standard Physical Property Measurement System (Model 6000, from Quantum Design) equipped with a vibrating sample magnetometer head. The measured sample was a commercial Sr-ferrite ( $\text{SrFe}_{12}\text{O}_{19}$ ) powder with a mass of 75 mg. Sr-ferrite is a hard magnetic material, i.e., high anisotropy material, with an anisotropy field close to 1.8 T and

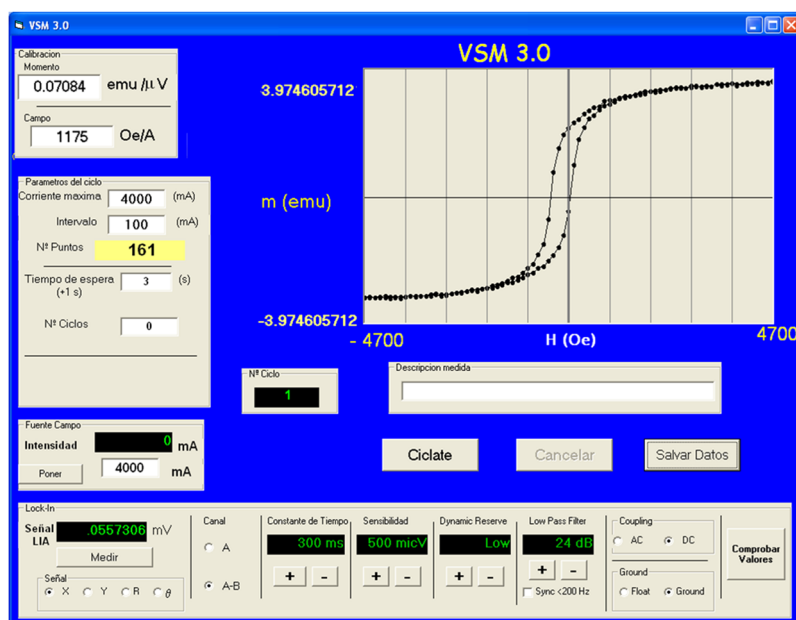


FIG. 6. Photo of the interface of VSM control program.

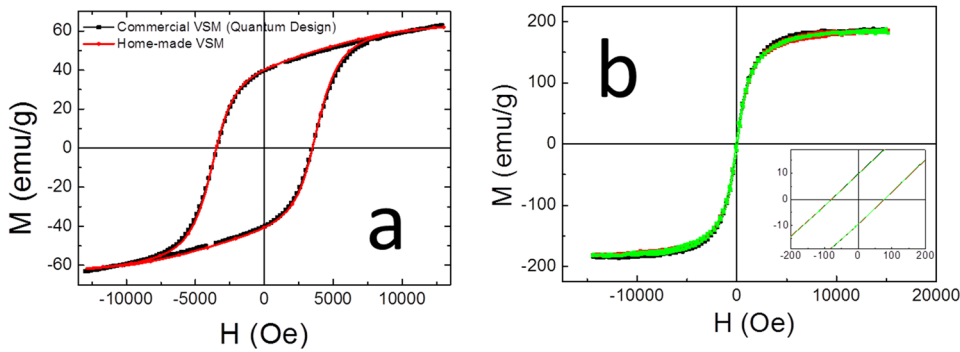


FIG. 7. (a) Magnetization curves at 300 K for a  $\text{SrFe}_{12}\text{O}_{19}$  isotropic powder sample obtained with our home-made setup and a commercial VSM from Quantum Design. (b) Consecutive magnetization curves for a 20 mg commercial Fe powder sample. Inset shows perfect overlap of the 3 consecutive curves at low fields.

a coercivity typically of the order of 2000–4000 Oe, depending on its microstructure. Figure 7(a) shows the result where both curves match in the whole range of measured fields demonstrating the reliability of our device. In addition, we measured 3 consecutive magnetization curves of an Fe powder sample (20 mg) in order to demonstrate both reproducibility and versatility, as Fe is a soft magnetic material. As Fig. 7(b) illustrates, the curves are perfectly reproducible, demonstrating that the system is free of drifts or any other time dependent spurious effects and that it can reliably measure both hard and soft magnetic materials.

In summary, the model of VSM we present here is simple and can be adapted to the specific type of materials to be studied depending on their magnetization, dimensions, and saturation field. When properly calibrated, the VSM provides accurate magnetization curves at room temperature. This model can be useful for both educational and research purposes.

## ACKNOWLEDGMENTS

This work has been supported by the Ministerio Español de Economía y Competitividad (MINECO), MAT2015-67557-C2-1-P, S2013/MIT-2850 NANOFRONTMAG, and by the European Commission through the project AMPHIBIAN (No. H2020-NMBP-2016-720853). V.L.D and M.A.G. acknowledge financial support from BBVA foundation.

Brian Richter (GMW Associates) is acknowledged for providing data on field uniformity.

- <sup>1</sup>B. D. Cullity and C. D. Graham, *Introduction to Magnetic Materials* (Wiley-IEEE Press, 2008).
- <sup>2</sup>G. C. Hadjipanayis and G. A. Prinz, *Science and Technology of Nanostructured Magnetic Materials* (Springer Science and Business Media, 2013).
- <sup>3</sup>O. Gutfleisch, M. A. Willard, E. Brück, C. H. Chen, S. G. Sankar, and J. Ping Liu, *Adv. Mater.* **23**, 821 (2011).
- <sup>4</sup>S. Foner, *Rev. Sci. Instrum.* **30**, 548 (1959).
- <sup>5</sup>A. Zieba and S. Foner, *Rev. Sci. Instrum.* **53**, 1344 (1982).
- <sup>6</sup>S. Foner, *J. Appl. Phys.* **79**, 4740 (1996).
- <sup>7</sup>S. Foner, *Rev. Sci. Instrum.* **46**, 1425 (1975).
- <sup>8</sup>J. A. Gerber, W. L. Burmester, and D. J. Sellmyer, *Rev. Sci. Instrum.* **53**, 691 (1982).
- <sup>9</sup>S. Nagata, E. Fujita, S. Ebisu, and S. Taniguchi, *Jpn. J. Appl. Phys., Part 1* **26**, 92 (1987).
- <sup>10</sup>M. Springford, J. R. Stockton, and W. R. Wampler, *J. Phys. E: Sci. Instrum.* **4**, 1036 (1971).
- <sup>11</sup>S. Foner and E. J. McNiff, Jr., *Rev. Sci. Instrum.* **39**, 171 (1968).
- <sup>12</sup>D. Dufeu, E. Eyraud, and P. Lethuillier, *Rev. Sci. Instrum.* **71**, 458 (2000).
- <sup>13</sup>R. P. Guertin and S. Foner, *Rev. Sci. Instrum.* **45**, 863 (1974).
- <sup>14</sup>W. Burgei, M. J. Pechan, and H. Jaeger, *Am. J. Phys.* **71**, 825 (2003).
- <sup>15</sup>See [http://www.gmw.com/electromagnets/dipole/3470/3470\\_Specs.html](http://www.gmw.com/electromagnets/dipole/3470/3470_Specs.html) for spatial field distribution curves for different configurations.
- <sup>16</sup>S. R. Trout, *IEEE Trans. Magn.* **24**, 2108 (1988).
- <sup>17</sup>G. J. Bowden, *J. Phys. E: Sci. Instrum.* **5**, 1115 (1972).
- <sup>18</sup>S. Tumanski, *Meas. Sci. Technol.* **18**, R31 (2007).
- <sup>19</sup>J. P. C. Bernardis, *Rev. Sci. Instrum.* **64**, 1918 (1993).
- <sup>20</sup>E. O. Samwel, T. Bolhuis, and J. C. Lodder, *Rev. Sci. Instrum.* **69**, 3204 (1998).